ELSEVIER

Pattern Recognition Letters 22 (2001) 813–823

Pattern Recognition Letters

www.elsevier.nl/locate/patrec

Error propagation for the Hough transform

Qiang Ji [a,*], Robert M. Haralick [b]

[a] *Department of Electrical, Computer, and Systems Engineering, Rensselaer Polytechnic Institute, Troy, NY 12180, USA*
[b] *Department of Electrical Engineering, University of Washington, USA*

Received 26 June 2000; received in revised form 25 December 2000

Abstract

In this paper, a statistically efficient Hough transform (HT) technique with improved performance in accuracy and robustness is described. The proposed technique analytically computes the uncertainty of each feature point based on image noise, the procedure used for estimating edge orientation, and the specific parametric representation scheme of a line. Using the estimated uncertainty of each feature point, a Bayesian probabilistic scheme is introduced to compute the contribution of each feature point to the accumulator. A performance evaluation of our technique reveals its improved performance, especially for noisy images.

Keywords: Hough transform; Line detection; Error propagation

1. Introduction

The Hough transform (HT) is a method for detecting straight lines and curves on gray level images. For line detection, the equation of a line can be expressed as

$$\rho = x\cos(\theta) + y\sin(\theta), \tag{1}$$

where θ and ρ are the line orientation and the distance from origin to the line, respectively. A line is therefore, completely specified by a parameter pair (θ, ρ). For straight line detection, the HT maps each edge pixel (x, y) from the image space into a parameter space of (θ, ρ), where contributions from each feature point to each possible set of (θ, ρ) are accrued. For this purpose the parameter space is divided into cells with each cell corresponding to a pair of quantized (θ, ρ). A multi-dimensional accumulator array is often used to represent the quantized space. For each feature point, all the parameters associated with the point are estimated, the corresponding cells of the accumulator are incremented accordingly. This is repeated for all feature points. Lines are found by searching the accumulator array for peaks. The peaks correspond to the parameters of the most likely lines.

The standard HT adopts a *top hat* strategy to compute the contribution of each point to a hypothesized line. Specifically, the scheme assumes all feature points located within a close range of the hypothesized line contribute equally to the line. The accumulator is, therefore, incremented by a unit for those feature points. This scheme is inadequate in that data points are not all equally reliable. By that, we mean the line parameters derived from each feature point may carry different

* Corresponding author.
E-mail address: qji@ecse.rpi.edu (Q. Ji).

0167-8655/01/$ - see front matter
PII: S0167-8655(01)00026-5

uncertainties due to the following reasons. Most HT techniques employ certain techniques for estimating the orientation of feature points (edgels) to restrict the ranges of values of θ a pixel may vote for. The estimation of the orientation of each edge pixel is often uncertain due to: (1) image noise (e.g., positional errors from quantization and sensor errors); (2) small neighborhood associated with the edge detection procedure and the inherent uncertainty with the procedure; (3) the parametric representation used to define a line (e.g., Eq. (1)). Feature points, therefore, vary in uncertainties. They should not be treated equally.

In this paper, we propose to investigate the efficacy of a probabilistic scheme for computing the contribution of each feature point to the accumulator array. Our scheme analytically estimates the uncertainty of the line parameters derived from each feature point, based on which a Bayesian accumulator updating scheme is proposed to compute the contribution of the point to the accumulator.

The proposed scheme is based on the following observation. At each edge pixel (x, y), its direction θ is first estimated based on the gradient information. The random perturbation on the input image data propagates to $\hat{\theta}$, the estimate of θ. The amount of uncertainty with $\hat{\theta}$ not only depends on image error but also on the procedure used to estimate $\hat{\theta}$. Subsequently, when ρ is computed based on $\hat{\theta}$ using Eq. (1), the perturbation on $\hat{\theta}$ propagates to $\hat{\rho}$, the estimate of ρ. The contribution of point (x, y) to parameter set $(\hat{\theta}, \hat{\rho})$, therefore depends on the uncertainty associated with $(\hat{\theta}, \hat{\rho})$. We propose to analytically estimate the uncertainty of each point and update the accumulator array accordingly based on the estimated uncertainty.

In the sections to follow, we detail the scheme and study its performance. Section 2 briefly discusses previous efforts in this area. The proposed scheme is covered in Section 3, where we analytically derive the error propagation scheme and the Bayesian accumulator updating scheme. Section 4 presents the results of a performance analysis of the improved HT against the standard HT transform. This paper ends in Section 5 with a discussion of the proposed scheme.

2. Previous work

Previous efforts in algorithmic improvement to HT focused on improving the computational efficiency of the HT (speed and memory). Early efforts in this aspect concentrated on reducing the number of bins used for tessellating the parameter space. Many proposed techniques drew on some form of coarse-to-fine search strategy resulting in a dramatic reduction of cells.

More recent efforts have been focusing on sampling the feature points. The idea is to use only a subset of image features. These efforts give rise to different probabilistic (also called randomized) HT techniques (Davies, 1986; Xu et al., 1990; Xu and Oja, 1993; Kiryati et al., 1991; Kalviainen et al., 1994; Galmbos et al., 1999), which increase the computational efficiency and decrease memory usage by means of sampling the image feature space.

Recently, Kittler and Pamler (1994) argued that research efforts should focus on addressing the issues of performance quality (accuracy) instead of on computational aspects. They believe that improvements in computer hardware automatically speed up algorithms, and that memory chips are becoming increasingly cheaper. We agree with their opinion. The emphasis of this research is therefore, on improving the robustness and accuracy of the HT techniques.

Researchers have long realized the limitation of the standard HT scheme and have proposed different schemes to improve the performance of HT. O'Gorman and Clowes (1976) first suggested the accumulator be increment by the magnitude of the gradient of each edge pixel. Their motivation is to weight the contribution of each edge pixel to the accumulator such that the pixels at which θ can be more accurately estimated contribute more to the accumulator. Other authors including Ballard (1981), Thrift and Dunn (1983), Veen and Groen (1991) suggest using weighting factors to weigh each feature point so that the most prominent or the most certain image features contribute more to accumulator cells than less certain data. Most of these schemes usually are variants of that of O'Gorman's, i.e., the weighting factors are derived from edge gradient

measurements. They are either ad hoc or heuristic, involving little theoretical justification. They ignored the uncertainties associated with the estimated ρ parameter. Furthermore, they tend to ignore the uncertainties introduced by the specific line parameter representation. As we will see, the uncertainties with ρ not only relate to gradient information but also relate to point location and line orientation. Thrift and Dunn (1983) proposed to use a heuristic function, called an *influence function*, to determine the contribution of each cell to the accumulator. The method was reported to be superior to the standard HT on noise perturbed examples of simple shapes. Haralick and Shapiro (1992) proposed a Bayesian approach to increment the accumulator based on the joint probability of θ and ρ, but did not elaborate on how the joint probability can be estimated.

Kittler and Pamler (1994) described a statistical hypothesis testing approach for the HT. The proposed technique replaces the commonly used top-hat kernel with a smooth kernel. For each feature point, its contribution to the accumulator array at a hypothesized cell (θ, ρ) is computed from the smooth kernel function, which is a function of the differences between the estimated model parameters and hypothesized model parameters.

Though very similar to our approach in spirit, they proposed a rather complex and computationally intensive scheme to derive an optimal analytic form of the kernel function. The kernel function is analytically determined by maximizing the power function, the probability of rejecting the incorrect hypothesis.

Stephens' (1991) work is very much similar to ours. Both methods update the accumulator array probabilistically. The major difference between ours and Stephens' lies in the probability used to update the accumulator. Through error propagation, we propagate the perturbation with each point to the computed curve parameter and update the true (quantized) curve parameter by its likelihood, assuming the computed curve parameter is Gaussian distributed with each quantized curve parameter as its mean and its perturbation (estimated via error propagation) as its covariance matrix. Stephens', on the other hand, only updates the computed curve parameter based on its likelihood given a point. It has the following drawbacks: (1) only the computed curve parameters are updated and others are not; (2) it is difficult to model the probability density function (pdf) between an image point and the estimated curve parameters. The proposed pdf model may be suitable for modeling the pdf of an image point with the ideal curve parameters. The two methods also differ in modeling perturbations with the image points. We model both intensity and positional errors while Stephens' only models positional error. Finally, Stephens did not mention for real images how to estimate the required positional and orientational errors.

3. Overview of the proposed scheme

We follow most HT techniques, i.e., starting with estimating θ for each pixel using directional intensity gradient measurements and then, computing ρ using Eq. (1). This can be used to restrict the range of values of θ that the pixel may vote for. It permits one-to-many mapping to be restricted to one-to-few mapping of image point to a parameter point. We assume that the gradient at a particular pixel is estimated by computing an equally weighted least squares fit to the gray levels in the pixel's neighborhood. It is also assumed that the input image is corrupted with additive Gaussian noise with zero mean and variance σ^2. In the following sections, we will show how to estimate θ for each pixel, compute its perturbation $\sigma_{\hat{\theta}}^2$, and analytically propagate this propagation to ρ.

3.1. Uncertainty of the estimated line parameters

Let $\hat{\Theta} = (\hat{\theta}, \hat{\rho})$ be a vector representing the estimated line parameters for a feature point. The uncertainty of the estimated line parameters can be characterized by $\Sigma_{\hat{\Theta}}$, the covariance matrix of $\hat{\Theta}$. $\Sigma_{\hat{\Theta}}$ can be analytically expressed as

$$\Sigma_{\hat{\Theta}} = \begin{pmatrix} \sigma_{\hat{\theta}}^2 & \sigma_{\theta\rho} \\ \sigma_{\theta\rho} & \sigma_{\hat{\rho}}^2 \end{pmatrix}, \tag{2}$$

where σ_θ^2 and σ_ρ^2 represent the variances of the estimated line orientation and position parameters, and $\sigma_{\theta\rho}$ the covariance of $\hat{\rho}$ and $\hat{\theta}$.

In the paragraphs to follow, we will show, how to analytically compute σ_θ^2, σ_ρ^2 and $\sigma_{\rho\theta}$, respectively.

3.1.1. Estimation of θ and its perturbation

If we approximate the image gray-tone values in pixel (x,y)'s neighborhood by a facet plane $\alpha y + \beta x + \gamma$ (Haralick, 1980), then the estimated gradient direction $\hat{\theta}$ for (x,y) is

$$\tan\hat{\theta} = \frac{\hat{\alpha}}{\hat{\beta}}, \tag{3}$$

where $\hat{\alpha}$ and $\hat{\beta}$ are estimates of α and β, resulting from a least-squares fitting. Taking a Taylor expansion of the right-hand side of Eq. (3) around (α,β), we obtain to a first order approximation

$$\Delta\tan\theta = \frac{1}{\beta}\Delta\alpha - \frac{\alpha}{\beta^2}\Delta\beta. \tag{4}$$

Similarly, expanding the left-hand side of Eq. (3) around θ, we obtain

$$\Delta\tan\theta = \frac{\Delta\theta}{\cos^2\theta}. \tag{5}$$

Combining Eqs. (4) and (5) yields

$$\Delta\theta = \left(\frac{1}{\beta}\Delta\alpha - \frac{\alpha}{\beta^2}\Delta\beta\right)\cos^2\theta. \tag{6}$$

As a result, the perturbation of $\hat{\theta}$, σ_θ^2, is

$$\sigma_\theta^2 = \left(\frac{\sigma_\alpha^2}{\beta^2} + \frac{\alpha^2\sigma_\beta^2}{\beta^4} - \frac{2\alpha}{\beta^3}\sigma_{\alpha\beta}\right)\cos^4\theta, \tag{7}$$

where α, β, σ_α^2, σ_β^2, and $\sigma_{\alpha\beta}$ are estimated as follows (Haralick, 1980). Let R be the rectangular region that we use to estimate α and β. Let the row index of R be Y and column index be X. And let $g(x,y)$ be the intensity at location (x,y). Then, we have $(x,y) \in X \times Y$.

$$\hat{\alpha} = \frac{\sum_{y\in Y}\sum_{x\in X} xg(x,y)}{\sum_{x\in X}\sum_{y\in Y} x^2}, \tag{8}$$

$$\hat{\beta} = \frac{\sum_{y\in Y}\sum_{x\in X} yg(x,y)}{\sum_{x\in X}\sum_{y\in Y} y^2}, \tag{9}$$

$$\sigma_\alpha^2 = \frac{\sigma^2}{\sum_{y\in Y}\sum_{x\in X} x^2}, \tag{10}$$

$$\sigma_\beta^2 = \frac{\sigma^2}{\sum_{y\in Y}\sum_{x\in X} y^2}, \tag{11}$$

$$\sigma_{\alpha\beta} = \frac{\sigma^2\sum_{y\in Y}\sum_{x\in X} xy}{\sum_{y\in Y}\sum_{x\in X} x^2\sum_{y\in Y}\sum_{x\in X} y^2}, \tag{12}$$

where $\sigma^2/(\sum_{y\in Y}\sum_{x\in X} y^2)$ and $\sigma^2/(\sum_{y\in Y}\sum_{x\in X} x^2)$ is the summation of the squared row (column) index values over the neighborhood used in the least-square fit. For a rectangular neighborhood, $\sigma_\alpha^2 = \sigma_\beta^2$. For a symmetric neighborhood R, that is, if $x \in R$ implies $-x \in R$, we have, $\sum_{y\in Y}\sum_{x\in X} xy = 0$, i.e., $\sigma_{\alpha\beta} = 0$.

We must emphasize two things. First, Eq. (7) only approximates variance of $\hat{\theta}$ estimated from the linear facet-fitting procedure. For $\hat{\theta}$ estimated from different procedures like Sobel or Canny, Eq. (7) is not applicable. This, however, does not mean we cannot propagate error for other edge detectors. In fact, for any edge detectors with a given kernel, we can analytically compute the uncertainties associated with the computed first order directional gradients (e.g., I_x and I_y) (Ji and Haralick, 1999a). Substituting α and β in equation with I_x and I_y in Eq. (3), we can proceed in the same fashion to compute σ_θ^2 and σ_ρ^2. Second, σ_θ^2 only characterizes the *random* uncertainties of $\hat{\theta}$ due to image noise σ^2. It does not account for any systematic errors inherent with the procedure used for estimating θ.

3.1.2. Estimating σ_ρ^2, the uncertainty of the estimated line parameter ρ

For each observed pixel (x,y), given $\hat{\theta}$ its $\hat{\rho}$ is estimated via

$$\hat{\rho} = x\cos\hat{\theta} + y\sin\hat{\theta}. \tag{13}$$

Taking a Taylor expansion of Eq. (13) around θ, x and y, we obtain to a first order approximation:

$$\Delta\rho = \cos\theta\Delta x + \sin\theta\Delta y + (y\cos\theta - x\sin\theta)\Delta\theta. \quad (14)$$

The variance of $\hat{\rho}$ is therefore,

$$\sigma_\rho^2 = \cos^2\theta\sigma_x^2 + \sin^2\theta\sigma_y^2 + (y\cos\theta - x\sin\theta)^2\sigma_\theta^2, \quad (15)$$

where σ_x^2, σ_y^2 and σ_θ^2 are standard deviations for positional and orientational errors. If we assume $\sigma_x^2 = \sigma_y^2 = \sigma_{\mathrm{p}}^2$, Eq. (15) becomes

$$\sigma_\rho^2 = \sigma_{\mathrm{p}}^2 + (y\cos\theta - x\sin\theta)^2\sigma_\theta^2.$$

If we let

$$k = y\cos\theta - x\sin\theta.$$

Then the variance of $\hat{\rho}$ is

$$\sigma_\rho^2 = k^2\sigma_\theta^2 + \sigma_{\mathrm{p}}^2. \quad (16)$$

By substituting Eq. (7) into (16), we have

$$\sigma_\rho^2 = k^2\left(\frac{\sigma_\alpha^2}{\beta^2} + \frac{\alpha^2\sigma_\beta^2}{\beta^4} - \frac{2\alpha}{\beta^2}\sigma_{\alpha\beta}\right)\cos^4\theta + \sigma_{\mathrm{p}}^2 \quad (17)$$

where α, β, σ_α^2, and σ_β^2 can be estimated from Eqs. (8)–(12), respectively. Geometrically, k can be interpreted as the distance from an image point (x, y) to the point closest to the origin on the line determined by (θ, ρ) as shown in Fig. 1. So σ_ρ^2 not only depends on σ_θ^2 but also on the geometric location of the point via k as well as line orientation. As k increases or θ decreases, σ_ρ^2 increases. It is also clear from Eq. (17) that σ_ρ^2 is a function of: (1) image intensity perturbation via σ_α^2, σ_β^2, and $\sigma_{\alpha\beta}$; (2) point location via k; (3) positional error via σ_{p}^2.

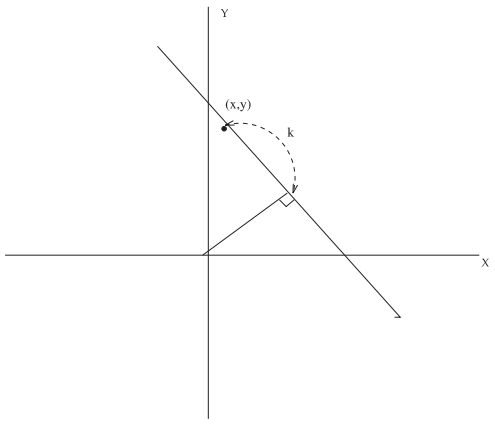

Fig. 1. Geometric interpretation of k.

Eq. (17) is significant in that it reveals that the variance of the estimated line parameter $\hat{\rho}$ not only relates to the input perturbation via perturbation on θ as expected, but also relates to the distance of the feature point to the origin (or the location of the point), as well as to the orientation of the line. It implies that a point further from the origin may induce more uncertainty and that lines with larger angles can be more accurately estimated than those with smaller angles. Given equal position, σ_ρ^2 is 0 for horizontal lines and is maximum for vertical lines. This echoes the conclusion drawn by Davies (1986), who showed that the parameter error increases as the distance from the foot of the normal to the origin increases. He recommended to change origins in order to derive more accurate parameter estimation.

This means that the uncertainty of a feature point depends on the HT coordinate system employed and that we can always translate and rotate the coordinate system to minimize σ_ρ^2. Based on the above analysis, we can conclude that the quality of the estimated line parameters can always be improved by simply selecting the appropriate coordinate system. A coordinate system centered at the centroid of the feature points should always yield better quality of the estimated line parameters than a coordinate system centered at one of the corners since it leads to smaller k value for each point.

Using Eq. (14), $\sigma_{\rho\theta}$, the covariance of $\hat{\rho}$ and $\hat{\theta}$ can be computed as follows.

$$\begin{aligned}\sigma_{\rho\theta} &= E(\Delta\theta\Delta\rho)\\ &= E[(\Delta\theta)^2](y\cos\theta - x\sin\theta)\\ &\quad + E[\Delta x\Delta\theta] + E[\Delta y\Delta\theta]\\ &= k\sigma_\theta^2, \end{aligned} \quad (18)$$

where we assume $\Delta\theta$ is uncorrelated to Δx and Δy.

3.2. Estimating image error σ^2

Computation of the σ_θ^2, σ_ρ^2, and $\sigma_{\theta\rho}$ requires σ^2, the amount of perturbation associated with image intensities. Let $\hat{I}(x, y)$ be the observed gray-tone

value for pixel located at (x,y). If we approximate the image gray-tone values in pixel (x,y)'s neighborhood by a plane $\alpha y + \beta x + \gamma$, then the image perturbation model can be described as

$$\hat{I}(x,y) = \alpha y + \beta x + \gamma + \xi,$$

where ξ represents the image intensity error and follows an iid distribution with $\xi \sim N(0,\sigma^2)$.

For a $M \times N$ neighborhood, the sum of squared residual fitting errors

$$\epsilon^2 = \sum_{y=1}^{N}\sum_{x=1}^{M}(\hat{I}(x,y) - \alpha x - \beta y - \gamma)^2,$$

is distributed $\sigma^2\epsilon^2 \sim \chi^2_{M\times N-2}$. As a result, we can obtain $\hat{\sigma}^2$, an estimate of σ^2, as follows

$$\hat{\sigma}^2 = \frac{\epsilon^2}{M \times N - 2}.$$

Assume each pixel is perturbed identically and independently with the same variance σ^2, we can obtain a more accurate estimate of σ^2 by averaging $\hat{\sigma}^2$ obtained from each neighborhood over the entire image.

Let $\hat{\sigma}_k^2$ be an estimate of σ^2 from the kth neighborhood. Given a total of K neighborhoods across the image, we can obtain

$$\hat{\sigma}^2 = \frac{1}{K}\sum_{k=1}^{K}\hat{\sigma}_k^2.$$

4. Increment the accumulator

Given $\Sigma_{\hat{\Theta}}$, we propose a Bayesian scheme to probabilistically compute the contribution of each feature point to the accumulator array. Assume $\hat{\Theta} = (\hat{\theta},\hat{\rho})$, a line parameter vector estimated from a feature point, is distributed as $\hat{\Theta} \sim N(\Theta, \Sigma_{\hat{\Theta}})$, where $\Theta = (\theta,\rho)$ is a vector consisting of all possible quantized values of θ and ρ. Given $\hat{\Theta}$, the likelihood of Θ can be computed as $P(\hat{\Theta}|\Theta)$

$$P(\hat{\Theta}\,|\,\Theta) = (2\pi)^{-1}|\Sigma_{\hat{\Theta}}|^{-1/2}\exp^{-(1/2)(\hat{\Theta}-\Theta)^t\Sigma_{\hat{\Theta}}^{-1}(\hat{\Theta}-\Theta)}. \tag{19}$$

If the prior information about Θ is available, then accumulator $H(\theta,\rho)$ for parameter $\Theta = (\theta,\rho)$ can be incremented by $P(\Theta\,|\,\hat{\Theta})$, the sum of posterior probability of Θ given $\hat{\Theta}$ at each image point (x,y), i.e.,

$$H(\Theta) = \Sigma_{(x,y)\in X\times Y}P(\Theta\,|\,\hat{\Theta}), \tag{20}$$

where $X \times Y$ is the image domain, note $\hat{\Theta}$ is a function of image point (x,y). If, however, the prior for Θ is not available, we may assume uniform prior for Θ, then $H(\theta,\rho)$ can be incremented by the sum of its likelihoods at each point, i.e.,

$$H(\Theta) = \Sigma_{(x,y)\in X\times Y}P(\hat{\Theta}\,|\,\Theta) \tag{21}$$

Given each image point, we can obtain an $\hat{\Theta}$, whose support for Θ is quantified by $P(\hat{\Theta}|\Theta)$. The total support for a particular quantized value Θ is the sum of all supports it receives from each every feature point.

It is clear from Eq. (21) that given each $(\hat{\theta},\hat{\rho})$ and its covariance matrix $\Sigma_{\hat{\Theta}}$, the bin for a (θ,ρ) is updated based on $P(\hat{\Theta}\,|\,\Theta)$, the likelihood of Θ given the observed $\hat{\Theta}$. The further away Θ is from $\hat{\Theta}$, the smaller the likelihood is and the less contribution $\Theta = (\theta,\rho)$ receives from the point (x,y) as shown in Fig. 2, which graphically illustrates the density function of $P(\hat{\Theta}\,|\,\Theta)$ given $\hat{\Theta}$ and $\Sigma_{\hat{\Theta}}$. The probabilistic updating scheme introduced here differs from the standard HT and other techniques in that, not only is $\Theta = \hat{\Theta}$ updated but other Θs

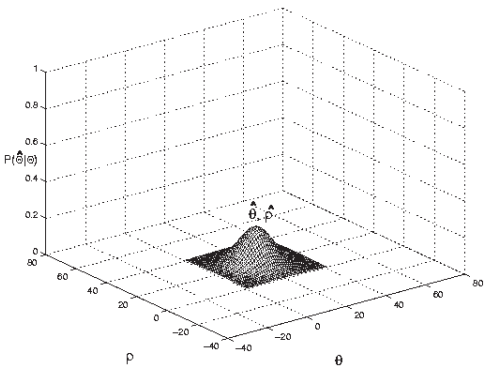

Fig. 2. Illustration of the procedure for probabilistically updating the accumulator array in the Hough space, where $\Theta = (\theta,\rho)$ is a quantized parameter and $P(\hat{\Theta}\,|\,\Theta)$ is the likelihood of Θ given $\hat{\Theta} = (\hat{\theta},\hat{\rho})$. $\hat{\Theta}$ is obtained from a feature point using Eq. (1).

nearby are also updated in a statistically optimal fashion.

The smooth kernel function as represented by $P(\hat{\Theta}\,|\,\Theta)$ is in firm contrast with the top-hat kernel employed by most HT techniques. While similar to the one proposed by Kittler and Pamler (1994), ours can be derived more efficiently.

In practice, given $\hat{\Theta}$ and its covariance matrix $\Sigma_{\hat{\Theta}}$, a 1σ-limit elliptical region can be established in $\theta - \rho$ space (the shaded region shown in Fig. 3) such that bins for Θs located within the shaded region are updated accordingly using Eq. (21) while bins for Θs located outside the region are not updated since their probabilities are negligible. The major and minor axes of the elliptical region are the two eigenvectors of $\Sigma_{\hat{\Theta}}$.

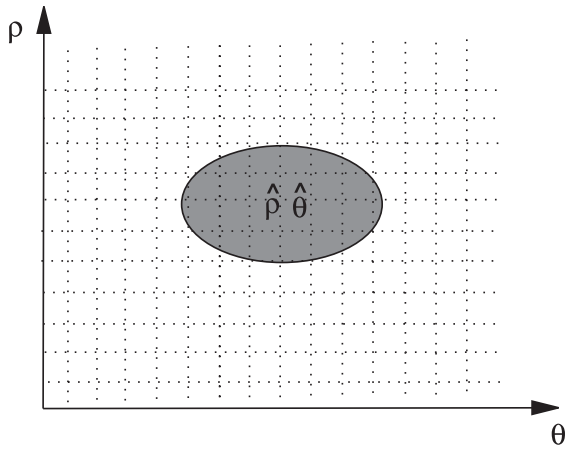

Fig. 3. An elliptical region for probabilistically updating the accumulator array in the Hough space.

5. Performance characterization

In this section, we present sample results on a variety of images to highlight the improvements in detection accuracy and robustness that can be obtained from the proposed scheme. The performance of the proposed scheme (referred to as improved HT hereafter) was evaluated against the standard HT on a synthetic image. Finally, the performance of the improved HT is further assessed using real images. The synthetic image contains a set of line segments in different directions as shown in Fig. 4. We are interested in comparing the results of the two methods by applying them to images corrupted with varying amount noises. The noisy images result from corrupting the intensities of original images by adding Gaussian noise with a mean of zero and a variance of σ^2 to each pixel independently. Three different values of σ^2 was used to perturb the original image. The edge points were extracted using a 3×3 facet model. The performance of a HT was evaluated by visually inspecting the 3D accumulator plots to see if distinct peaks can be recognized. These peaks correspond to the line segments in the image.

5.1. Experimental results

The first part of the experiment involves 3D accumulator plots comparison. The accumulator array obtained using the standard and improved HT on perfect images are plotted in Figs. 5(a) and (b), respectively. The two images look very much identical (though the peaks in (b) are more

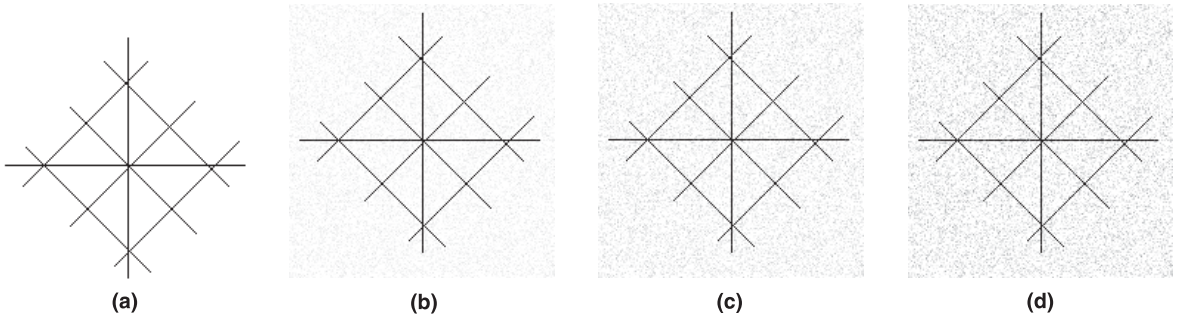

Fig. 4. The synthetic test image containing eight lines segments: (a) the original image; (b) image after perturbing (a) with $\sigma = 5$; (c) image after perturbing (a) with $\sigma = 10$; (d) image after perturbing (a) with $\sigma = 20$.

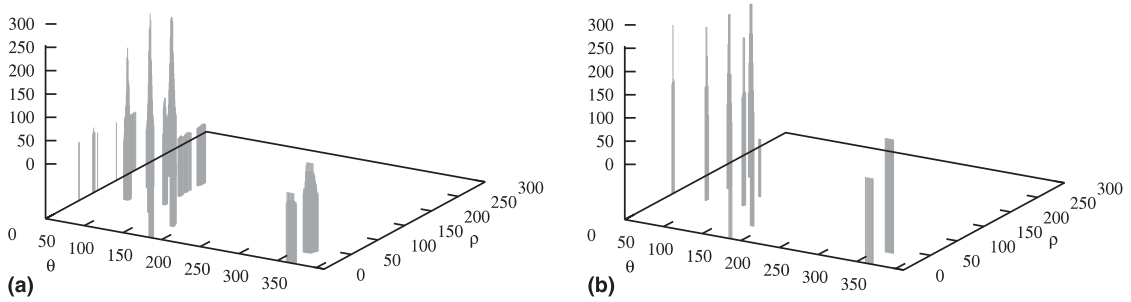

Fig. 5. 3D accumulator plots obtained using the standard HT (a) and the improved HT (b) from the perfect image. The eight peaks correspond to the eight line segments in the image.

distinctive). This is correct since when $\sigma^2 = 0$, we can see from Eq. (17), the variance of ρ is zero. The improved scheme is therefore the same as the standard HT. Figs. 6–8 show the accumulator arrays obtained using the improved HT and standard HT, respectively on noisy images, with $\sigma^2 = 5$, 10 and 20, respectively. From these figures, we can see as the noise level increases, the performance of standard HT degenerates very quickly as shown by the larger blurred peak clusters, a reduction in the number of peaks observable, and an increase in the number spurious peaks. For example, when $\sigma^2 = 10$, only three peaks can be recognized from Fig. 7(a) and there are several false peaks near 0°, 315° and 360°. The problem is more evident in Fig. 8(a), with a significant

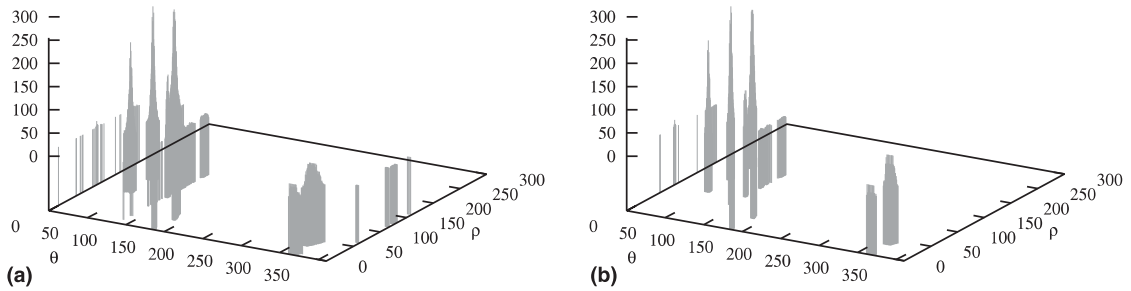

Fig. 6. 3D accumulator plots obtained using the standard HT (a) and the improved HT (b) from the image corrupted with noise level of $\sigma = 5$.

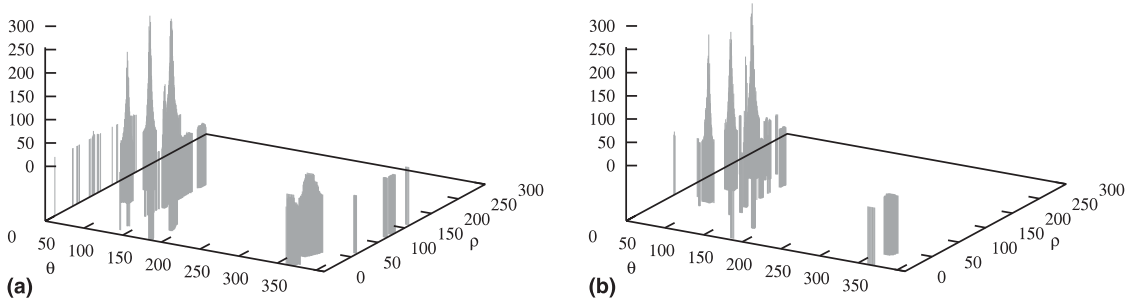

Fig. 7. 3D accumulator plots obtained using the standard HT (a) and the improved HT (b) from the image corrupted with noise level of $\sigma = 10$.

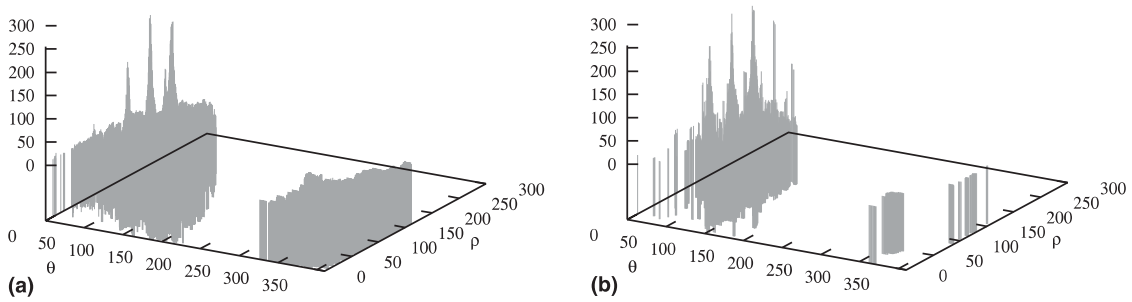

Fig. 8. 3D accumulator plots obtained using the standard HT (a) and the improved HT (b) from the image corrupted with noise level of $\sigma = 20$.

increase in spurious peaks and resulting in a loss of half of the line segments and peaks become even more indistinguishable. In contrast, for the improved HT, the effect of additional noise is not as much serious as shown in Figs. 7(b) and 8(b). Similar results were obtained when using other synthetic images. To test our technique with real images, we applied it to images parts. Sample results are shown in Figs. 9 and 10.

6. Discussion and future work

In this paper, we introduce a Bayesian updating scheme that systematically ties the uncertainties computed for each point to its contribution. The contribution of each point to a (θ, ρ) is proportional to its likelihood. The proposed scheme is based on an analytical propagation of input errors. It results from theoretical and statistical derivations and therefore, possesses a great statistical efficiency.

Our study shows that the uncertainty of a feature point depends on: (1) the input perturbation; (2) its relative spatial location to the Hough coordinate system; (3) edge detector; (4) line representation scheme. We can always manipulate the HT coordinate system to reduce the uncertainty with each feature point, therefore, improving the quality of the estimated line parameters. This implies that a HT coordinate system centered at the centroid of the image feature should yield better line parameter estimates than a coordinate system centered at one of the corners.

The preliminary results from the performance characterization of the proposed scheme on

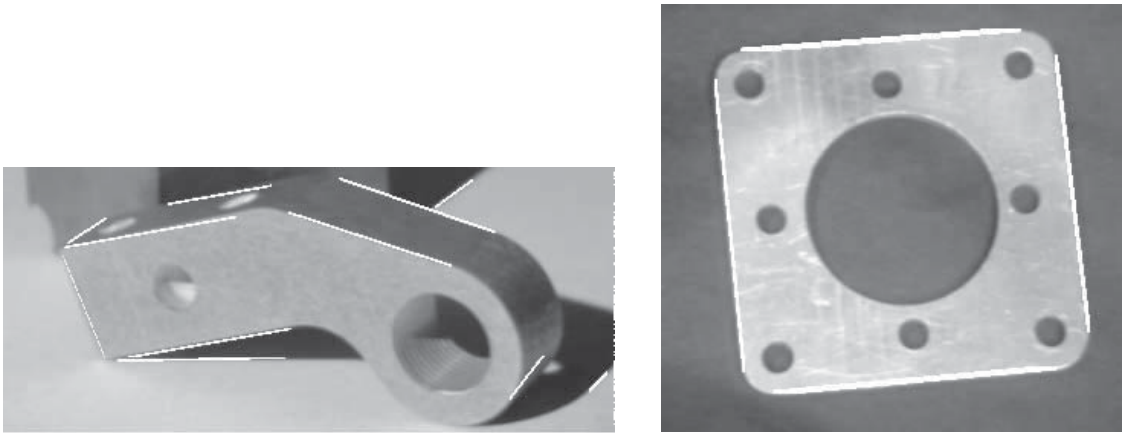

Fig. 9. Examples of detected lines for two real images. Detected lines are superimposed on the original images.

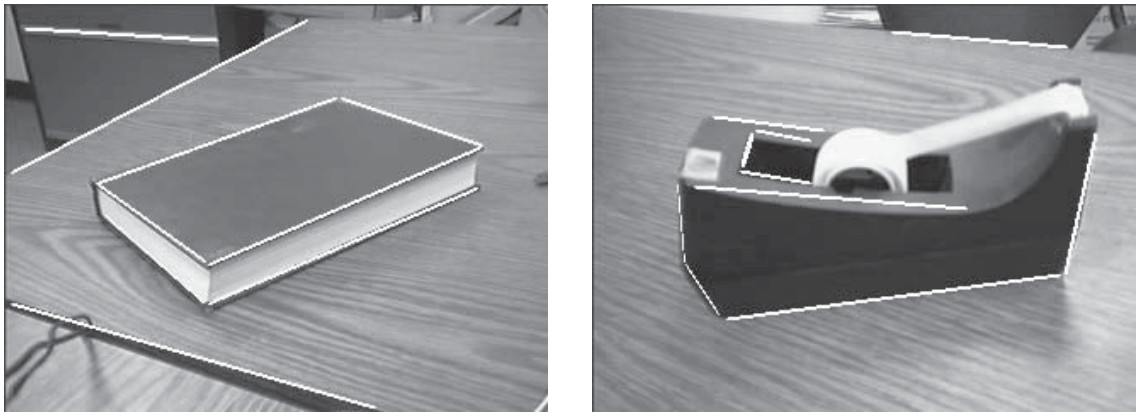

Fig. 10. Examples of detected lines for two additional images. Detected lines are superimposed on the original images.

synthetic images revealed that the proposed scheme is superior to the standard HT in that it can yield a better accumulator with less irrelevant data and more prominent peaks, especially in noisy images. The study also shows that the improved HT is more robust and accurate to noise and yields good results with real images.

A further advantage of the proposed method is that it quantifies the uncertainties associated with the estimated line parameters. This valuable information can be subsequently exploited by the higher vision tasks to characterize the accuracy of its output.

One disadvantage of the proposed scheme as compared to the standard HT is that it is computationally more involved. This problem will become less an issue with the advent of the new computer hardware. Another disadvantage of our approach is that it ties to the technique used for estimating edge orientation. For a different edge-orientation technique, the error propagation procedure needs to be re-derived to compute the variance of the estimated edge orientation. However, basic theory for error propagation with most edge detectors like Canny and Sobel can be derived in a similar fashion. Furthermore, error propagation from θ to ρ and the Bayesian scheme for incrementing the accumulator remain the same. Another potential disadvantage with our approach as with any HT that makes use of the edgel orientation computed from an edge detector, the systematic positional error (bias) associated with the estimated edgel orientation is not accounted for. Our approach implicitly assumes small systematic positional error. The systematic positional error could be large for certain edge detectors operating with small convolution kernel. We only consider random positional error.

One of the future tasks is to conduct experiments to compare the proposed scheme with other methods, especially the one proposed by Kittler and Pamler (1994). From Eq. (17), we can see σ_ρ^2 depends on k. Minimizing k can therefore, reduce the uncertainties associated with each edge point. For a given image, k can be minimized by selecting the origin of HT coordinate at the centroid of the objects of interests (here are linear features). As a result, another possible future work is to verify the impact of different HT coordinate systems on HT performance including accuracy and computational complexity.

The error propagation scheme discussed in this paper is only intended for least-square line fitting. We have, however, extended (Ji and Haralick, 1999b) this scheme to allow analytical error propagation for general curve-fitting problems including circles and ellipses. Given the covariance matrix characterizing the error of the estimated curve parameters, the Bayesian accumulator updating scheme introduced in this paper can be directly applied. We can therefore, conclude that the extended error propagation scheme can be used with the HT for detecting any curves.

References

Ballard, D.H., 1981. Generalizing the Hough transform to detect arbitrary shapes. Pattern Recognition 13, 111–122.

Davies, E.R., 1986. Image space transforms for detecting straight edges in industrial images. Pattern Recognition Lett. 4, 185.

Galmbos, C., Matas, J., Kittler, J., 1999. Progressive probabilistic Hough transform for line detection. In: 1999 IEEE Comput. Soc. Conf. Comput. Vision Pattern Recognition, pp. 554–560.

Haralick, R.M., 1980. Edge and region analysis for digital image data. CGIP 12, 60.

Haralick, R.M., Shapiro, L.G., 1992. Computer and Robot Vision. Vol. 1, Addison-Wesley, Reading, MA, p. 585.

Ji, Q., Haralick, R., 1999a. Quantitative evaluation of edge detectors using the minimum kernel variance criterion. In: IEEE Internat. Conf. Image Processing, Kobe, Japan, October, pp. 705–709.

Ji, Q., Haralick, R.M., 1999b. Error propagation for computer vision performance characterization. In: Internat. Conf. Imaging Science, Systems, and Technology, Las Vegas, June, pp. 429–435.

Kalviainen, H., Hirvonen, P., Xu, L., Oja, E., 1994. Comparisons of probabilistic and non-probabilistic Hough transforms. In: Proc. 3rd European Conf. Comput. Vision, 2–6 May, 1994, p. 801.

Kiryati, N., Eldar, Y., Bruckstein, A.M., 1991. Probabilistic Hough transform. Pattern Recognition Lett. 24 (4), 303–316.

Kittler, J., Pamler, P.L., 1994. Robust and statistically efficient detection of parametric curves in 2d images. NSF/ARPA Workshop on Performance and Methodology in Computer Vision, Seattle.

O'Gorman, F., Clowes, M.B., 1976. Finding picture edges through collinearity of feature points. IEEE Trans. Comput. C-25 (4), 449.

Stephens, R.S., 1991. Probabilistic approach to the Hough transform. Image Vision Comput. 9 (1), 66–71.

Thrift, P.R., Dunn, S.M., 1983. Approximating point-set images by line segments using a variation of the Hough transform. Comput. Vision Graphics Image 21, 383.

Veen, T.M., Groen, F.C., 1991. Discretization errors in the Hough transform. Pattern Recognition 14 (1–6), 137.

Xu, L., Oja, E., 1993. Randomized Hough transform: basic mechanisms, algorithms, and computational complexities. CVGIP: Image Understanding 57 (2), 131–154.

Xu, L., Oja, E., Kultanen, P., 1990. A new curve detection method: randomized Hough transform (rht). Pattern Recognition Lett. 11 (5), 331–338.